arXiv:1602.01692v1 [nucl-th] 4 Feb 2016

New Astrophysical Reaction Rate for the $^{12}C(\alpha,\gamma)^{16}O$ Reaction

Zhen-Dong An[1,2], Yu-Gang Ma[1,3], Gong-Tao Fan[1], Yong-Jiang Li[1], Zhen-Peng Chen[4], and Ye-Ying Sun[5]

1. Shanghai Institute of Applied Physics, Chinese Academy of Sciences, Shanghai 201800, China

2. University of Chinese Academy of Sciences, Beijing 100049, China

3. ShanghaiTech University, Shanghai 200031, China

4. Department of Physics, Tsinghua University, Beijing 100084, China

5. Department of Materials, Tsinghua University, Beijing 100084, China

Email: ygma@sinap.ac.cn

Email: zhpchen@tsinghua.edu.cn

Received _____; accepted _____

ABSTRACT

A new astrophysical reaction rate for $^{12}C(\alpha,\gamma)^{16}O$ has been evaluated on the basis of a global R-matrix fitting to the available experimental data. The reaction rates of $^{12}C(\alpha,\gamma)^{16}O$ for stellar temperatures between $0.04 \leq T_9 \leq 10$ are provided in a tabular form and by an analytical fitting expression. At $T_9 = 0.2$, the reaction rate is $(7.83 \pm 0.35)\times10^{15}$ cm^{3}mol^{-1}s^{-1}, where stellar helium burning occurs.

Subject headings: nuclear reactions, nucleosynthesis, abundances – Galaxy: abundances – stars: evolution – stars: abundances – supernovae: general

1. Introduction

Astrophysical reaction rates are of great importance in studies of the stellar nucleosynthesis and the stellar evolution. During stellar helium burning the rates of 3α and $^{12}C(\alpha,\gamma)^{16}O$ reaction, in competition with one another, determine the time scale of this phase and the relative abundances of ^{12}C and ^{16}O in a massive star. The reaction rate of 3α process is known to have an uncertainty about 10% (Fynbo et al. 2005), at the astrophysical temperatures (0.2×10^9 K); while such accuracy is not the case for $^{12}C(\alpha,\gamma)^{16}O$reaction yet relevant for the rise time of the type I supernova light curves (Dominguez et al. 2001), the production of important radioactive nuclei ^{26}Al, ^{44}Ti, and ^{60}Fe (Tur et al. 2010), the size and mass of Fe core for a pre-supernova star (Woosley et al. 2003), and the formation of X-ray black hole binaries (Brown et al. 2001) and neutron star (Brown et al. 1998; Wen & Zhou 2013) in massive stars.

Experimental investigations on the reaction rate $N_A\langle\sigma v\rangle$ are calculated with the following standard formula (Rolfs & Rodney 1988),

$$N_A\langle\sigma v\rangle = \Big(\frac{8}{\pi\mu}\Big)^{1/2}\frac{N_A}{(k_BT)^{3/2}}\times\int_0^\infty dES(E)\exp(-\sqrt{\frac{E_G}{E}}-\frac{E}{k_BT}), \quad (1)$$

where N_A refers to the Avogadro's constant, μ is the reduced mass of entrance channel $^{12}C+\alpha$, k_B is the Boltzmann constant, and $E_G=(2\pi\alpha Z_\alpha Z_C)^2\mu c^2/2$ is the Gamow energy with the fine-structure constant α. The function S(E)= $\sigma(E)E\exp(2\pi\eta)$ is the total S factor of $^{12}C(\alpha,\gamma)^{16}O$, where $\eta=Z_\alpha Z_C e^2/(\hbar\nu)$ is the Sommerfeld parameter, and $\sigma(E)$ is the cross section. For each temperature of T_9 (temperature in units of 10^9 K), the rate is obtained by Eq.(1) with corresponding data of the S(E) factor.

The difficulty in measuring the S factor of $^{12}C(\alpha,\gamma)^{16}O$ reaction results from the extremely small $\sigma(E_0)$, which is about 10^{-17} b at 0.3 MeV, where the helium burning occurs. The observed S(E) factors are focused on the energy region of $E_{c.m.}>0.9$ MeV, which

means that an extrapolation cannot be evaded at the present. It remains a challenging task to obtain the S(E) factor for the $^{12}C(\alpha,\gamma)^{16}O$ reaction in part due to the complicated level structure of ^{16}O nucleus (deBoer et al. 2013; Ma et al. 2014).

The $^{12}C(\alpha,\gamma)^{16}O$ reaction rates at astrophysical temperatures are dominated by resonances states in the compound nucleus ^{16}O. The rates based upon the different extrapolation and fitting models to the parts of existing S(E) factors measurements, such as the potential models and R-matrix (or K-matrix) theory, were reported by several research teams. Representative results for the rates from R-matrix (or K-matrix) theory were provided by Caughlan & Fowler (1988) (hereafter CF88), Buchmann (1996), Angulo et al. (1999) (hereafter NACRE), and Kunz et al. (2002). Two recent compilations, Katsuma (2012) and Xu et al. (2013) (hereafter NACRE II), are mainly based on the potential models. However, for the corresponding reaction rate at $T_9 = 0.2$ of these compilations, the published S-factor at 0.3 MeV disagrees at the 10% level (see Table 1 of An et al. (2015)) with the quoted uncertainties about twice as large as estimated for precision modeling efforts (Woosley & Heger 2007).

In An et al. (2015), we report a reduced R-matrix theory to make the global fitting to plenty of complementary experimental data about the ^{16}O compound nucleus. These complementary data effectively help us to understand the concrete effect of the ^{16}O nucleus for the S(E) factor and the reaction rate. Based on the published S factor estimates, the updated astrophysical reaction rates of $^{12}C(\alpha,\gamma)^{16}O$ are presented and compared with the previous published reaction rates in this paper.

2. Reaction Rates

2.1. The uncertainty of S-factors

The S factors of $^{12}C(\alpha,\gamma)^{16}O$ is constituted by several resonant peaks with strong interference pattern. And the complicated mechanism of this reaction results in unpredictable interference effects from the first principles (Kunz et al. 2002). The global fitting for ^{16}O system with a multilevel, multichannel R-matrix allows simultaneous analysis of differential cross section data and angle-integrated cross section of ^{16}O compound nucleus (An et al. 2015). Multichannel R-matrix analysis provides the possibility of reducing the uncertainties in the extrapolated total and partial S factors of $^{12}C(\alpha,\ \gamma)^{16}O$ reaction, and the interpretation of interference mechanism via additional constraint offered by the simultaneous analysis of multiple reaction channels (Azuma et al. 2010).

The error propagation formulae (Smith 1991) are adopted to determine the uncertainty of the S factor in the whole energy region. Our extrapolation value is $S_{tot}(0.3\ MeV) = 162.7\pm7.3$ keV b, which is composed of $S_{E10}(0.3\ MeV) = 98.0\pm7.0$ keV b, $S_{E20}(0.3\ MeV) = 56.0\pm4.1$ keV b ground state captures and of cascade captures, $S_{casc}(0.3\ MeV) = 8.7\pm1.8$ keV b. And the cascade transition of $S_{6.05}$ and $S_{6.13}$ at 0.3 MeV are 4.91 ± 1.11 keV.b and 0.16 ± 0.26 keV b, respectively. They are quite consistent with the constructive interference result of $S_{6.05}(0.3\ MeV) = 4.36 \pm 0.45$ keV.b and destructive interference of $S_{6.13}(0.3\ MeV) = 0.12 \pm 0.04$ keV b of Avila et al. (2015), which constrained contribution of the values by measuring the asymptotic normalization coefficients (ANCs) for these states using the α-transfer reaction $^{6}Li(^{12}C,\ d)^{16}O$. We adopt a similar approach for the fitting of cascade transitions. This is one of the reasons that uncertainty of the extrapolated S factor reduces dramatically. The values of other two cascade transitions are $S_{7.12}(0.3\ MeV) = 0.63 \pm 0.22$ keV b and $S_{6.92}(0.3\ MeV) = 3.00 \pm 0.42$ keV b, which are in excellent agreement with recent results of Schürmann et al. (2012), respectively.

2.2. New reaction rate for $^{12}C(\alpha,\gamma)^{16}O$

The absolute values of reaction rates, $N_A\langle\sigma v\rangle$ of $^{12}C(\alpha,\gamma)^{16}O$ can be obtained by the Eq.(1) from the self-consistent total S factor and its uncertainties. Table 1 lists 80 points of reaction rates in the temperature range of $0.04 \leq T_9 \leq 10$. To be precise, the total reaction rate of $^{12}C(\alpha,\gamma)^{16}O$ is achieved after multiplying $N_A\langle\sigma v\rangle$ with the probability densities of the reaction partners and integrating over the energy interval. The uncertainties of the reaction rates obtained from our R-Matrix model are also tabulated for the high and the low rate in Table 1.

According to the Gamow theory (Rolfs & Rodney 1988), for the nonresonant cross section, the Gamow window (significant integral interval) of each T_9 is selected in $[E_0 - \Delta E_0/2,\ E_0 + \Delta E_0/2]$, with $E_0=(E_G^{1/2}k_BT/2)^{2/3}$ and $\Delta E_0=(16E_0k_BT/3)^{1/2}$. Considering typical T_9 temperatures involved, we have $E_0 = 0.3$ MeV of helium-burning start at $T_9 = 0.2$. And for the S factor data, the chief center-of-mass energy range is 0.1-0.5 MeV. As E_0 and ΔE_0 increase with stellar temperature, the S(E) factor data in the higher energy range play a leading role gradually for the reaction rate.

To understand influence of the S(E) factor of $^{12}C(\alpha,\gamma)^{16}O$ on the reaction rate at different temperatures, probability density functions of the total reaction rates at T_9 = 0.2, 1.0, 2.0, 3.0, 4.0, 5.0, 6.0, 8.0 and 10.0 are shown in Fig.1. At $T_9 = 0.2$ and 1.0, the probability density functions are located almost in the extrapolated S factor, without resonance peaks, so the Gamow window can be well approximated by a Gaussian-distribution with the most effective energy $E_0 = 0.3$ MeV and $E_0 = 0.9$ MeV. As the T_9 increases from 1 to 10, however, the influence of resonances of S(E) factor becomes more and more remarkable, and the probability density functions can no longer be approximated by the Gaussian-distribution. So, $^{12}C(\alpha,\gamma)^{16}O$ reaction rate at these temperatures can be obtained just by the S factor measurements at energies as wide as possible.

The S_{tot} measurements of Schürmann et al. (2005, 2011), in reverse kinematics using the recoil mass separator allowed to acquire data with a high degree of accuracy (<3%) in a wide energy scope of $E_{c.m.}$ = 1.5 - 4.9 MeV. These data would make good restriction to probability density functions of T_9 = 2.0, 3.0, and 4.0 (Fig. 1C-1E), and uncertainties of $^{12}C(\alpha,\gamma)^{16}O$ reaction rate are smaller than 3% from $2.0 \leq T_9 \leq 4.0$.

Kunz et al. (2002) studied on the S factor to the ground state of $^{12}C(\alpha,\gamma)^{16}O$ at higher energies, covering the 1_3^- ($E_{c.m.}$= 5.28 MeV) and 1_4^- ($E_{c.m.}$= 5.93 MeV), using resonance parameters of Tilley et al. (1993) in the calculation. The published data in two independent experiments (Ophel et al. 1976; Brochard et al. 1973) of the ground-state transition were neglected. Possible interference effects were included in the calculation of S_{E10} and S_{E20} by applying the R-matrix fitting procedures, but they were somewhat speculative, and the results of $S_{g.s}$ were about 2∼5 times away from experimental data. Therefore, from the probability density functions of T_9 = 5.0, 6.0, 8.0 and 10.0 (Fig. 1F-1I), it can be inferred that the rate calculation of Kunz et al. (2002) is significantly higher.

The S_{tot} can be indicated according to different types of J^π (0^+, 1^-, 2^+, 3^-, and 4^+). Fig. 2(A) shows the fractional contributions of different values of J^π to the total reaction rates in $0.04 \leq T_9 \leq 10.0$. It can be seen that $J^\pi = 1^-$ and 2^+ dominate the reaction rate up to T_9 = 2.0. From the probability density functions of T_9 = 0.2, 1.0, and 2.0 (Fig. 1A-1C), we note that the contribution stems mainly from $J^\pi = 1^-$ ($E_{c.m.}$= 2.42 MeV) and $J^\pi = 2^+$ ($E_{c.m.}$= 2.58 MeV) levels in ^{16}O. The rate above T_9 = 2.0, the fraction from 3^- gradually increases with temperature. This comes from the contribution of $J^\pi = 3^-$ ($E_{c.m.}$= 4.44, 5.97, and 6.10 MeV) resonances. The contribution of $J^\pi = 4^+$ increases with T_9 first, and then decreases, having two 4^+ resonances just at $E_{c.m.}$= 3.20 and 3.93 MeV in integral interval. Thus, the fractional contributions of different values of J^π reconfirmed the validity of the probability density functions in Fig. 1.

The contributions of ground state capture and cascade captures to the reaction rate of $^{12}C(\alpha,\gamma)^{16}O$ are illustrated in Fig. 2(B). Ground state capture (S_{E10} and S_{E20}) dominates the reaction rate up to $T_9 = 0.1$. And the contributions from the cascade transitions increase with T_9. Beside at the important He-burning temperature $T_9 = 0.2$, the rate is still important all the way up to $T_9 = 5.0$, because the inverse reaction of $^{12}C(\alpha,\gamma)^{16}O$ plays an important role in silicon burning (Woosley 2013). So cascade transition is necessary to the precise calculation of reaction rate.

2.3. Comparison to Other $^{12}C(\alpha,\gamma)^{16}O$ Determinations

Fig. 3 shows comparisons between our new reaction rate and previous estimates. In each panel the dashed line shows the ratio of a previous determination to our new rate. The grey bands are the uncertainty of the published rate, e.g., in Fig. 3(A) the edges of grey zone are reaction rate ratios of NARCE II's limits to the principal value of our rates. The blue bands estimate the uncertainty of our rate. Below $T_9 \approx 4.0$, our recommended results are within the uncertainties of Buchmann (1996), Kunz et al. (2002) and NACRE II. Above $T_9 = 4$, the results agree with the analysis of NACRE.

By comparing all the published rates with our present results, the principal values of each rate are shown in Fig. 4. At astrophysical temperature of T_9 =0.2 the new rate is about 10% larger than the rate of NACRE II (S_{tot}(0.3 MeV)=148±27 keV b) and Buchmann (1996) (S_{tot}(0.3 MeV)=146 keV b), about 16% lower than the rate of the NACRE (S_{tot}(0.3 MeV)=199±64 keV b), and it is quite consistent with the adopted value of Kunz et al. (2002) (S_{tot}(0.3 MeV)=165±50 keV b).

In the intermediate range $0.5 \leq T_9 \leq 3$, our recommended rate is in good agreement with NACRE II. The temperature dependence of our recommended value differs significantly

from the rates of Katsuma (2012), which stems from the higher total S factor at 1_2^- ($E_{\rm c.m.}$= 2.42 MeV) resonance-peak, overestimating the cross-section of Schürmann et al. (2005) in their calculations (Katsuma 2008). In the same temperature range, the deviation from Kunz et al. (2002) mainly originates from the lower calculation values of total S factor from $E_{\rm c.m.}$= 0.5 MeV to $E_{\rm c.m.}$= 2.0 MeV. The lower value of NACRE is a direct consequence of the considered cascade transitions for the total S-factors.

For the rates above $T_9 = 3$, our reaction rate increases with T_9 but has lower values than Kunz et al. (2002) and NACRE II, because the high-energy data covering the 1_3^- and 1_4^- resonance are overestimated apparently in their calculations.

2.4. Analytical formula

A common form of reaction rate is an analytical formula with an appropriate parametrization for applications in stellar models. Eq. (2) is a usual expression (Buchmann 1996; Kunz et al. 2002).

$$N_{\rm A}\langle\sigma v\rangle^{AF} = \frac{a_0}{T_9^2(1+a_1T_9^{-2/3})^2}\exp\Big[-\frac{a_2}{T_9^{1/3}}-\Big(\frac{T_9}{a_3}\Big)^2\Big]+\frac{a_4}{T_9^2(1+a_5T_9^{-2/3})^2}\exp\Big(-\frac{a_6}{T_9^{1/3}}\Big)$$
$$+\frac{a_7}{T_9^{3/2}}\exp\Big(-\frac{a_8}{T_9}\Big)+\frac{a_9}{T_9^{2/3}}(1+a_{10}T_9^{1/3})\exp\Big(-\frac{a_{11}}{T_9^{1/3}}\Big). \qquad (2)$$

The difference between the fitting formula to tabulated rate is shown in Fig.3 (F). The blue bands indicate the uncertainty of adopted rate in Table 1. The dotted line shows the ratio of the adopted values of the analytical expression normalized to the adopted tabulated ones. It is applicable in temperature range of $0.04 \leq T_9 \leq 10$ with a maximum deviation of 4.0% to the recommended rate in Table 1. For the most important range of T_9 = 0.1-0.3 the maximal deviation is 1%. And the parameters $a_0 - a_{11}$ are $a_0 = 4.70 \times 10^8$; $a_1 = 0.312$; $a_2 = 31.8$; $a_3 = 400$; $a_4 = 1.08 \times 10^{15}$; $a_5 = 23.6$; $a_6 = 41.3$; $a_7 = 2.49 \times 10^3$; $a_8 = 28.5$; a_9

$= 1.19 \times 10^{11}$; a_{10} = -98.0; a_{11} = 36.5.

3. Conclusions

New $^{12}C(\alpha,\gamma)^{16}O$ reaction rates in the range of $0.04 \leq T_9 \leq 10$ have been estimated from recent S factor modeling. The measurements at higher energies are analyzed in our R-matrix fit, which significantly reduce the uncertainty of reaction rate at higher temperatures. A comprehensive comparison is done between our results and the previous data. It should be noted that, the results are obtained by theoretical extrapolation of existing experimental data of ^{16}O system. There could be some important factors that our model does not include. Additional experiments and theoretical work are needed to further validate existing expressions for the $^{12}C(\alpha,\gamma)^{16}O$ rate.

From the Figs. 1 and 2, it is suggested that an improved investigation of S_{casc} and S_{TOT} at 1_3^- and 1_4^- resonances, may help to further reduce the uncertainties of reaction rates at higher temperatures. Moreover, the asymptotic normalization coefficients (ANCs) of the corresponding states do not consist with each other in the transfer reaction (Brune et al. 1999; Belhout et al. 2007; Oulebsir et al. 2012; Avila et al. 2015) with big uncertainty, which remain to be solved. Finally, the extrapolated S_{tot}(0.3 MeV) is quite sensitive to the data as close as possible to the Gamow window. The reverse reaction (γ, α) using a high photon flux γ-ray beam, such as the High Intensity γ-ray Source at TUNL (Gai et al. 2012; DiGiovine et al. 2015) and the under construction of Shanghai Laser Electron Gamma Source facility in our team (Xu et al. 2007; Luo et al. 2011), would be desirable to allow a measurement of cross sections in the pb region.

The authors would like to thank Prof. Stan Woosley and Prof. Alexander Heger for helpful discussions of reaction rates. This work is supported partially by the National

Natural Science Foundation of China under Grant Nos. 11175233, 91126017 and 11421505 and the 973 project under contract no. 2014CB845401.

REFERENCES

An, Z. D., et al. 2015, PhRvC, 92, 045802

Angulo, C., Arnould, M., Rayet, M., et al. 1999, NuPhA, 656, 3 (NECRE)

Avila, M. L., Rogachev, G. V., et al. 2015, PhRvL, 114, 071101

Azuma, R. E., Uberseder, E., et al. 2010, PhRvC, 81, 045805

Belhout, A., Ouichaoui, S., Beaumevieille, H., et al. 2007, NuPhA, 793, 178

Brochard, F., Chevallier, P., Disdier, D., et al. 1973, J. Phys. France, 34, 363

Brown, E. F., & Bildsten, L. 1998, ApJ, 496, 915

Brown, G. E., Heger, A., Langer, N., et al. 2001, NewA, 6, 457

Brune, C. R., Geist, W. H., Kavanagh, R. W., et al. 1999, PhRvL, 83, 4025

Buchmann, L. 1996, ApJ, 468, L127

Caughlan, G. R., & Fowler, W. A. 1988, ADNDT, 40, 283 (CF88)

deBoer, R. J., et al. 2013, PhRvC, 87, 015802

DiGiovine, B., Henderson, D., et al. 2015, NIMPA, 781, 96

Dominguez, I., Höflich, P., & Straniero, O. 2001, ApJ, 557, 279

Fowler, W. A. 1984, RvMP, 56, 149

Fynbo, H. O. U., Diget, C. A., et al. 2005, Natur, 433, 136

Gai, M., et al., 2012, JPhCS, 337, 012054.

Katsuma, M. 2008, PhRvC, 78, 034606

Katsuma, M. 2012, ApJ, 745, 192

Kunz, R., Jaeger, M., Mayer, A., et al. 2002, ApJ, 567, 643

Luo, W., Xu, W., Pan, Q. Y., An, Z. D., et al. 2011, NIMPA, 660, 108

Ma, C. W., Lv, C. J., Wei, H. L., et al. 2014, NST, 25, 040501

Ophel, T. R., Frawley, A. D., Treacy, P. B., & Bray, K. H. 1976, NuPhA, 273, 397

Oulebsir, N., Hammache, F., Roussel, P., et al. 2012, PhRvC, 85, 035804

Rolfs, C. E., & Rodney, W. S. 1988, Cauldrons in the Cosmos (Chicago, IL: Univ. Chicago Press), pp. xi-xii.

Schürmann, D., Di Leva, A., De Cesare, N., et al. 2005, EPJA., 26, 301

Schürmann, D., Di Leva, A., Gialanella, L., et al. 2011, PhLB, 703, 557

Schürmann, D., Gialanella, L., Kunz, R., & Strieder, F. 2012, PhLB, 711, 35

Smith, D. L. 1991, Probability, Statistics, and Data Uncertainties in Nuclear Science and Technology (Amer Nuclear Society, Chicago).

Tilley, D. R., Weller, H. R., & Cheves, C. M. 1993, NuPhA, 564, 1

Tur, C., Heger, A., & Austin, S. 2010, ApJ, 718, 357

Wen, D. H., & Zhou, Y. 2013, NST, 24, 050508

Woosley, S. E., Heger, A., et al., 2003, NuPhA, 718, 3c

Woosley, S. E., & Heger, A. 2007, PhR, 442, 269

Woosley, S. E. 2013, private communication

Xu, Y., Xu, W., Ma, Y. G., et al. 2007, NIMPA, 581, 866

Xu, Y., Takahashi, K., Goriely, S., et al. 2013, NuPhA, 918, 61(NACREII)

This manuscript was prepared with the AAS LaTeX macros v5.2.

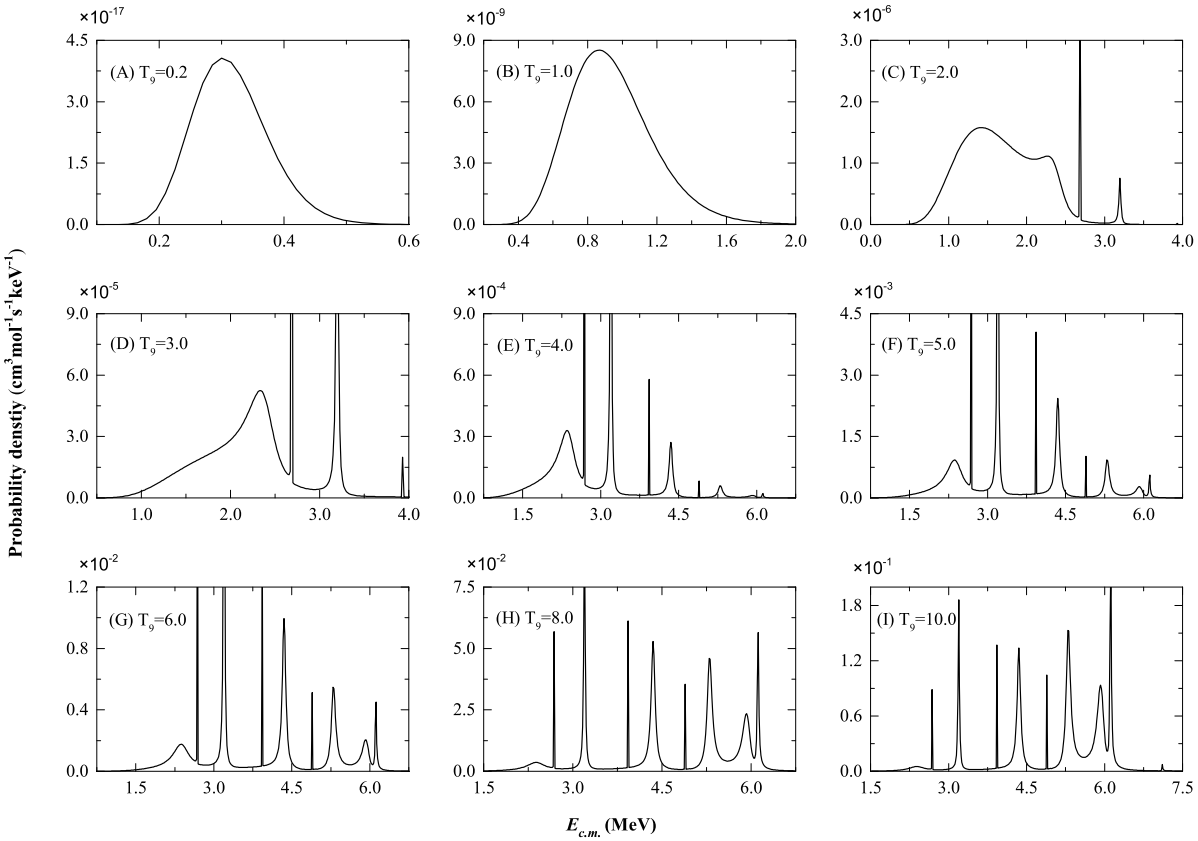

Fig. 1.— Reaction rate probability density functions for $^{12}\mathrm{C}(\alpha,\gamma)^{16}\mathrm{O}$ at different values of T_9.

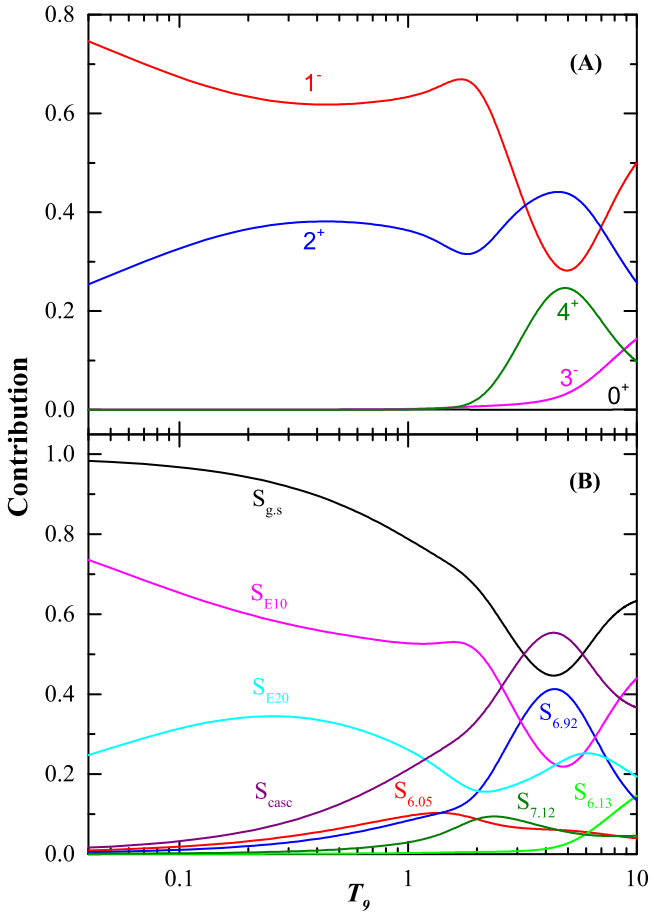

Fig. 2.— Top: fractional contributions of different J^{π} to the total reaction rates of $^{12}C(\alpha,\gamma)^{16}O$. Bottom: fractional contributions of $S_{g.s.}$ (including E_{10} and E_{20} to the ground state) and the cascade transitions to the total rates.

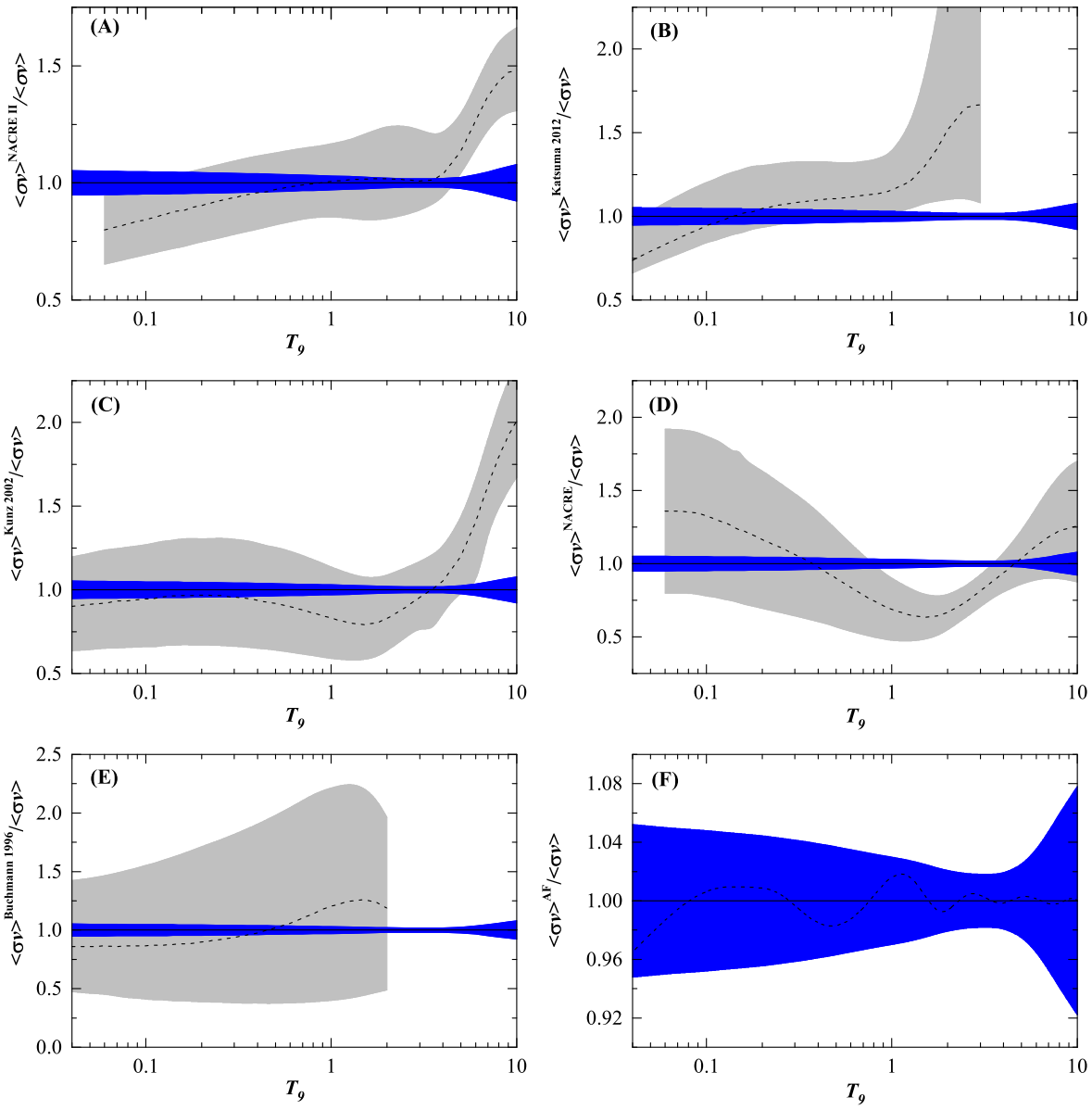

Fig. 3.— Comparisons (ratio) of $^{12}C(\alpha,\gamma)^{16}O$ reaction rates from the compilations of (A) NACRE II, (B) Katsuma (2012), (C) Kunz et al. 2002, (D) NACRE and (E) Buchmann (1996) with our new recommended rate. Accuracy of the analytic formula according to Eq.(2) is shown in Fig.3(F).

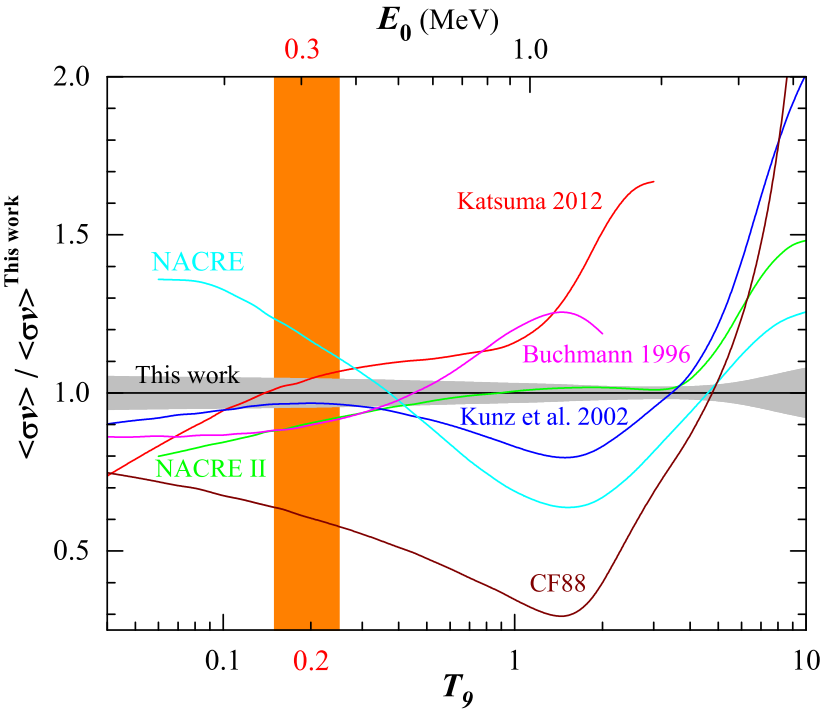

Fig. 4.— Comparisons of astrophysical reaction rate of $^{12}C(\alpha,\gamma)^{16}O$ (including CF88) normalized to our new recommended rate.

Table 1. The $^{12}C(\alpha,\gamma)^{16}O$ reaction rates (in $cm^3mol^{-1}s^{-1}$).

T_9	$N_A\langle\sigma v\rangle$	High	Low	10^n	T_9	$N_A\langle\sigma v\rangle$	High	Low	10^n
0.040	9.27	9.75	8.79	-31	0.60	3.28	3.40	3.17	-8
0.042	3.94	4.14	3.74	-30	0.65	8.00	8.27	7.73	-8
0.045	2.92	3.07	2.77	-29	0.70	1.78	1.84	1.73	-7
0.050	5.69	5.98	5.40	-28	0.75	3.70	3.82	3.58	-7
0.055	7.60	7.98	7.21	-27	0.80	7.19	7.42	6.96	-7
0.060	7.51	7.88	7.13	-26	0.85	1.32	1.37	1.28	-6
0.065	5.81	6.10	5.52	-25	0.90	2.33	2.40	2.26	-6
0.070	3.67	3.85	3.49	-24	0.95	3.93	4.05	3.81	-6
0.075	1.95	2.05	1.86	-23	1.00	6.41	6.60	6.22	-6
0.080	9.00	9.44	8.57	-23	1.10	1.56	1.60	1.51	-5
0.085	3.66	3.84	3.49	-22	1.20	3.42	3.52	3.33	-5
0.090	1.34	1.40	1.27	-21	1.30	6.96	7.15	6.78	-5
0.095	4.45	4.67	4.24	-21	1.40	1.33	1.36	1.30	-4
0.100	1.36	1.43	1.30	-20	1.50	2.41	2.47	2.35	-4
0.105	3.88	4.06	3.69	-20	1.60	4.19	4.29	4.09	-4
0.11	1.03	1.08	0.98	-19	1.70	7.02	7.18	6.85	-4
0.12	6.18	6.48	5.89	-19	1.80	1.14	1.16	1.11	-3
0.13	3.06	3.20	2.91	-18	1.90	1.80	1.83	1.76	-3
0.14	1.29	1.35	1.23	-17	2.00	2.76	2.82	2.71	-3
0.15	4.75	4.97	4.53	-17	2.10	4.15	4.23	4.07	-3
0.16	1.56	1.64	1.49	-16	2.20	6.10	6.22	5.98	-3

Table 1—Continued

T_9	$N_A\langle\sigma v\rangle$	High	Low	10^n	T_9	$N_A\langle\sigma v\rangle$	High	Low	10^n
0.17	4.67	4.88	4.46	-16	2.30	8.79	8.96	8.62	-3
0.18	1.28	1.34	1.23	-15	2.50	1.73	1.76	1.69	-2
0.19	3.27	3.42	3.13	-15	2.75	3.66	3.73	3.60	-2
0.20	7.83	8.18	7.48	-15	3.00	7.13	7.26	7.00	-2
0.21	1.77	1.85	1.69	-14	3.25	1.29	1.32	1.27	-1
0.22	3.79	3.96	3.63	-14	3.50	2.20	2.24	2.16	-1
0.24	1.53	1.59	1.46	-13	3.75	3.58	3.64	3.51	-1
0.26	5.29	5.52	5.07	-13	4.00	5.57	5.67	5.46	-1
0.28	1.62	1.69	1.55	-12	4.25	8.37	8.54	8.21	-1
0.30	4.47	4.66	4.29	-12	4.50	1.22	1.25	1.20	0
0.32	1.13	1.18	1.08	-11	5.00	2.42	2.48	2.36	0
0.34	2.65	2.75	2.54	-11	5.50	4.43	4.56	4.31	0
0.36	5.81	6.04	5.57	-11	6.00	7.60	7.87	7.34	0
0.38	1.20	1.25	1.15	-10	6.50	1.23	1.28	1.18	1
0.40	2.37	2.46	2.27	-10	7.00	1.90	1.99	1.81	1
0.42	4.46	4.63	4.28	-10	7.50	2.79	2.94	2.64	1
0.45	1.07	1.11	1.03	-9	8.00	3.95	4.18	3.71	1
0.50	3.91	4.05	3.76	-9	9.00	7.13	7.63	6.64	1
0.55	1.21	1.25	1.17	-8	10.0	1.15	1.24	1.06	2